Energy Engineering

Tech Science Press

https://doi.org/10.32604/ee.2026.078275

ARTICLE

Parametric Optimization of Battery Capacity and Electric Motor Power for Electric Vehicles under Varying Loads and Capacities

Ivan Pliško, Mihael Cipek* and Danijel Pavković

Faculty of Mechanical Engineering and Naval Architecture, University of Zagreb, Zagreb, Croatia

*Corresponding Author: Mihael Cipek. Email: mihael.cipek@fsb.unizg.hr

Received: 28 December 2025; Accepted: 28 February 2026; Published: 18 June 2026

ABSTRACT: Nowadays, battery electric vehicles are increasingly used, from passenger cars to heavy-duty commercial vehicles, trains, and ships, all in an effort to reduce greenhouse gas emissions. In electric vehicles, battery capacity significantly affects their range and performance, but a larger battery also increases the vehicle's mass and cost. This paper proposes parametric optimization of battery capacity and peak electric motor power for electric vehicles under different load types and vehicle capacities. A computational model of an electric vehicle is developed, with parameters such as battery capacity, payload, and peak motor power being variable. Using parametric optimization algorithms, the optimal electric vehicle configuration for different load types and battery capacities is determined. Based on the optimization results, the relationships between the parameters are analyzed, and a conclusion is presented.

KEYWORDS: Electric vehicles; battery capacity; motor power; parametric optimization; different load; computational model

1 Introduction

Electromobility has undergone robust development in recent years, driven primarily by the urgent need to decarbonize the transportation sector, which remains responsible for approximately 20% of global greenhouse gas (GHG) emissions [1]. To meet ambitious climate targets, such as the European Green Deal's objective of net-zero emissions by 2050, strict regulations have been introduced to phase out internal combustion engines, accelerating the shift toward sustainable transport solutions [2]. The drive towards greening of the transport sector, besides increasingly GHG emission regulations, is also facilitated by technological advancements in battery systems and the growing demand for sustainable transport [3]. Electric vehicles (EV) represent a key technology to a GHG-free future of the transport sector because they are characterized by high energy efficiency and zero GHG emissions, but at the same time, EVs still have certain limitations [4]. Those limitations include high initial costs, limited charging infrastructure, and driver range anxiety [5].

The driving range of an electric vehicle is fundamentally determined by the energy capacity of its battery [6]. However, increasing the battery capacity requires complex trade-offs in terms of increasing the vehicle mass, which, in turn, increases the vehicle energy consumption required to overcome the rolling resistance and inertia, as well as road grade, thus diminishing the effect of range increase [7]. Some of the more recent comparative studies emphasize that lighter vehicles often demonstrate superior economy performance, while heavier, long-range models require disproportionately larger battery packs to achieve similar range efficiency [8]. Moreover, optimizing the electric motor power ratings is equally critical to

vehicle performance. While higher electric machine power improves drivability and road grade negotiation, it also increases the cost of the powertrain in turn. Therefore, simultaneous parametric optimization of battery capacity and electric motor power is key to balancing the driving performance, cost, and efficiency under varying load conditions.

In EV research, different modelling and optimization approaches have been proposed to address these design challenges. For example, reference [9] focuses on high-fidelity electro-thermal (multi-physics) models that can be used to predict battery pack performance with rather high accuracy, whereas reference [10] analyzes vehicle dynamics and losses in the main electrical machine. Some recent studies have utilized multi-objective optimization algorithms, such as NSGA-II, to determine optimal powertrain configurations by considering variable efficiencies (described by two-dimensional efficiency maps) of the electric motor and inverter rather than using constant-valued efficiencies within the optimization process [11]. Moreover, data-driven approaches based on reinforcement learning have been explored recently to optimize energy management strategies in real-time [12]. Also, some contemporary studies focus on highly sophisticated estimation techniques, such as three-time-scale dual extended Kalman filtering for precise battery parameter and state monitoring [13]. However, complex models can be computationally demanding for preliminary design sizing. Special emphasis in optimization is often placed on the objective function, which must carefully balance investment costs against operating efficiency and penalties for failing to meet performance constraints [14]. To alleviate these computational burdens during preliminary stages, researchers are increasingly adopting surrogate modelling techniques. These methods replace expensive high-fidelity finite-element simulations with fast, data-driven approximations, enabling extensive multi-objective exploration without sacrificing system-level accuracy [15]. Furthermore, because isolated component sizing often leads to suboptimal overall vehicle performance, modern frameworks emphasize holistic co-optimization. These approaches evaluate the interdependent dynamics of the entire powertrain (incorporating the battery, motor, and transmission simultaneously) to guarantee optimal parameter matching under specific dynamic driving constraints [16]. Beyond static design sizing, operational parameters are actively managed by integrating advanced predictive control strategies, such as Model Predictive Control (MPC). MPC methodologies complement structural sizing by proactively anticipating power fluctuations and dynamically allocating energy, which significantly extends battery lifespan and improves overall system reliability [17].

The aim of this paper is to develop a simplified yet robust computational model for determining the optimal battery capacity and motor power of electric vehicles under varying load conditions. The proposed framework emphasizes computational efficiency, transparency, and interpretability. By focusing on fundamental physical laws rather than high-fidelity multi-physics discretization, the simulation time per driving cycle is reduced by several orders of magnitude compared to detailed electro-thermal or CFD-based approaches. While complex models may require minutes or hours per iteration, the simplified physics-based formulation allows for the evaluation of thousands of design candidates in a matter of seconds. This rapid execution makes the model particularly suitable for early-stage sizing and extensive parametric sensitivity studies, where the goal is to narrow down the design space before committing to computationally expensive high-fidelity validation. The results are based on two prominent electric vehicles that represent distinct vehicle classes and design philosophies: i.e., the Renault Zoe and the Tesla Model 3, wherein the former is a representative of subcompact (city) electric vehicles, whereas the latter would be classified as a mid-size electric sedan. The analysis is based on calculating the energy consumption during a particular driving profile [18], which is then translated to battery capacity and electric machine power ratings.

2 Methods

For the purposes of this research, a computer model of an electric vehicle was developed to estimate energy requirements, consumption and performance for different combinations of battery capacity, electric motor power and payload. The proposed model is intentionally simplified to facilitate large-scale parametric optimization through the DIRECT algorithm. By utilizing average efficiency and steady-state dynamics, the model achieves the computational speed required for global search. It is important to note the operational boundaries of this approach: mechanisms such as battery thermal dynamics, capacity fade due to aging, and voltage-swing-dependent losses are neglected. Consequently, the model is positioned as a tool for comparative design studies and preliminary sizing rather than high-fidelity energy prediction. For final-stage validation, the optimized configurations identified here should be subjected to high-fidelity multi-physics simulation to account for the aforementioned non-linearities.

2.1 Vehicle Dynamics

Rolling resistance force (F_{roll}) is a resistive force that opposes the motion of a rolling body:

$$F_{roll} = \mu_r mg, \tag{1}$$

where the rolling friction coefficient (μ_r) typically has a value of 0.01–0.015 and it depends on the tire type and the pressure inside of the tire [19]. The value 0.012 is chosen in this paper. The value for free fall acceleration is 9.81 m/s^2 [20].

Total mass (m) is defined as a sum of the empty vehicle mass (m_0), battery mass (m_{bat}) that is proportional to its capacity and the load mass (m_{load}). In this study, different load types (such as passengers, luggage, or commercial payload) are represented in an aggregated manner through the additional load mass m_{load}. This approach assumes that the primary influence of these loads on vehicle dynamics and energy consumption is captured via the total added mass, rather than through secondary effects like changes in the center of gravity or aerodynamics. Consequently, the load type is not explicitly modeled as a separate variable but is parameterized through m_{load} to maintain model simplicity and computational efficiency. In this way, the variable m_{load} indirectly affects the whole energy consumption and range of a vehicle. Renault Zoe has a curb weight of 1577 kg [21], and a battery that weights 326 kg [22], whereas Tesla Model 3 has a curb weight of 1760 kg [23], and a battery that weights 480 kg [24].

Aerodynamic drag (F_{aero}) is a loss that is generated because of the friction when an object moves through the air. It depends on the shape of an object [20] as follows:

$$F_{aero} = 0.5\rho C_d A v^2(t), \tag{2}$$

where ρ is the density of air (1.295 kg/m^3) [25], C_d is the aerodynamic drag factor that increases when a vehicle has a poorly designed aerodynamic shape (for regular cars C_d has a value of 0.3 [19]), A is the frontal area of a vehicle and v is vehicle velocity.

Note that the frontal area of Renault Zoe is approximately 2.79 m^2 [21], while Tesla Model 3 has a frontal area of 2.67 m^2 [23].

Hill climbing force (F_{hc}) is a force that is needed to drive the vehicle up a slope [19] as follows:

$$F_{hc} = mg \sin\theta, \tag{3}$$

where $\sin\theta$ corresponds to the slope grade which is defined as a ratio between changed height and changed distance and can be changed depending on the desired hill slope. For small angles $\sin\theta \approx \tan\theta \approx grade$.

In the basic simulation grade is equal to zero to avoid big energy results and too big consumption. Instead, hill climbing force is contained in the requirement to drive uphill through the "performance point". At a given speed and a given slope, the power of the drive is calculated then penalized. That approach keeps the consumption and the whole simulation on a realistic level and at the same time satisfies demanded grade.

As the vehicle speed changes over time, inertial force (F_{inert}) can be calculated based on the vehicle acceleration $a(t)$ as follows:

$$F_{inert} = ma\,(t)\,. \tag{4}$$

Traction force (F_{trac}) needs to overcome all aforementioned resistances to motion (Eqs. (1)–(3)) and the inertial force (Eq. (4)) during driving, and is therefore defined as [19]

$$F_{trac}\,(t) = F_{roll} + F_{aero} + F_{grade} + F_{inert}. \tag{5}$$

The required driveline mechanical power (P_{mech}) which needs to be provided must by the propulsion system can be calculated as [20]:

$$P_{mech}\,(t) = F_{trac}\,(t)\,v\,(t)\,, \tag{6}$$

where v is vehicle velocity in (m/s).

2.2 Electric Motor and Inverter Model

Electric vehicle motor torque T_m can be reconstructed from mechanical power and motor angular speed as follows [20]:

$$T_m\,(t) = \frac{P_{mech}\,(t)}{w_m}, \tag{7}$$

where w_m is the angular velocity that is equal to ratio of the vehicle velocity ($v(t)$) and the size of the tire, which is 0.33 m according to [26].

All the losses within the electric motor need to be accounted for. The following equation was adjusted and simplified, so the variables like torque can be directly used and minimized by replacing constants with coefficients [27] as follows:

$$P_{loss} = k_{fric} + k_{Cu}{T_m}^2 + k_{Fe}{w_m}^2, \tag{8}$$

where k_{fric} are the constant mechanical losses [W] representing friction in bearings, transmission and has a value of 400 [W], then $k_{Cu}{T_m}^2$ are the copper (ohmic) losses in the windings and the higher the torque, the higher the losses. The coefficient k_{Cu} has a value of $2 \cdot 10^{-3}$ W. The term $k_{Fe}{w_m}^2$ represents the iron losses that depend on the speed of rotation because they are caused by the change in magnetic flux in the cores. The coefficient k_{Fe} has a value of $2 \cdot 10^{-5}$ W. Coefficients (k_{fric}, k_{Cu} and k_{Fe}) are assumed parameters that physically correspond to different types of losses (friction, copper, iron). They are used because they provide a sufficiently precise, yet simple model for analyzing motor performance. These values are chosen so that the total losses (expressed in Watts) are within a realistic range.

Output drive power delivered to the inverter (equal to the sum of mechanical power and losses, limited by the maximum drive power) is given by:

$$P_{out} = \min\left(P_{mech}\,(t) + P_{loss}\,(t)\,, P_{max} \cdot 1000\right). \tag{9}$$

This considers that the drive system cannot deliver more power than its peak (rated) value [28]. DC power that battery needs to deliver to the inverter according to [20] is:

$$P_{dc}(t) = \frac{P_{out}(t)}{\eta_{inv}}, \tag{10}$$

where $P_{out}(t)$ is the output power (defined in Eq. (9)), and η_{inv} is the efficiency of the inverter. The efficiency of the inverter is usually above 95% [29]. In this paper the value for the efficiency of the inverter is selected to be 0.97.

2.3 Battery Model

The battery model is based on a simplified calculation of energy flow and state of charge (SoC). Momentary battery current ($I(t)$) (with auxiliary consumption (P_{aux}) that compensates all electric consumers that are not directly involved in drivetrain) is given by the derivative of the main formula for electrical power at DC bus [30]:

$$I(t) = \frac{P_{dc}(t) + P_{aux}}{V_{nom}}, \tag{11}$$

where $P_{dc}(t)$ is an DC power output with auxiliary consumption (P_{aux}) that compensates all electric consumers that are not directly involved in drivetrain. Auxiliary consumption (P_{aux}) has a value of 500 W [31]. Nominal voltage of the battery V_{nom} for Renault Zoe is 350 V, and for Tesla Model 3 is 357 V [32].

State of charge (SoC) is calculated iteratively for each simulation step (Coulomb Counting) [33] with the negative sign indicating the discharge regime of the EV battery:

$$SOC_{k+1} = SOC_k - \frac{I(t)\Delta t}{Q}, \tag{12}$$

where Q is the capacity of the battery, and k is the time step (time increment, with the simulation time step $\Delta t = 1$ s used in this work). The gradual discharge of the battery during the driving cycle is modelled in this way. The conversion of battery energy to capacity in ampere-hours (Ah) is based on the standard relationship Ah = Wh/V [34]. Battery charge capacity Q is defined in this study in the following way:

$$Q = \frac{E_{bat} \cdot f_{usable} \cdot 1000}{V_{nom}}, \tag{13}$$

where E_{bat} [kWh]is a nominal capacity of the battery, f_{usable} is the usable share of the battery charge (energy) and the value of the usable share is 0.9 [35]. Total battery capacity of Renault Zoe is 52.0 kWh, while Tesla Model 3 battery has a total battery capacity of 78.1 kWh [32].

The total energy drawn from the battery during the simulation ($E_{batt,out}$) in Watt-hours (Wh) is calculated as the sum of momentary values of DC power:

$$E_{batt,out} = \sum_k \max\left(P_{dc,k}\frac{\Delta t}{3600}, 0\right), \tag{14}$$

where $P_{dc,k}$ is the current power that battery delivers at simulation step k. It includes the power required for the motor and inverter, motor and inverter losses and auxiliary consumption. The factor 1/3600 converts [Ws] to [Wh]. Max operator ensures that only discharge energy accumulates, while regenerative breaking is not considered (conservative assumption). In standardized driving cycles such as WLTC, regenerative

braking can significantly reduce net energy consumption, particularly in urban and transient phases characterized by frequent decelerations. The inclusion of regenerative braking would primarily reduce the total energy drawn from the battery and, consequently, increase the achievable driving range for a given battery capacity. As a result, incorporating regenerative braking into the model would likely shift the optimization results toward lower optimal battery capacities, especially for smaller vehicles. While this simplification may reduce quantitative accuracy when compared to real-world operation, it ensures conservative sizing and computational efficiency in early stages of vehicle design.

2.4 Specific Consumption and Range

The total energy consumption during the driving cycle (E_{cons}) is calculated as the sum of the momentary DC power delivered by the battery to the inverter:

$$E_{cons} = \sum_t P_{dc}(t)\frac{\Delta t}{3600}, \tag{15}$$

where $P_{dc}(t)$ is the instantaneous DC power delivered by the battery to the inverter. Δt is the simulation time step in seconds. While $E_{batt,out}$ gives a realistic estimate of how much energy is actually drawn from the battery (without returning energy), E_{cons} represents the total energy required by the system to move the vehicle during the driving cycle.

The travelled distance (s) is calculated as the integral of the vehicle velocity over time:

$$s = \int_0^T v\,(t)\,dt. \tag{16}$$

Specific consumption is defined based on the total energy consumption and travelled distance [36] as follows:

$$spec = \frac{E_{cons}}{s}. \tag{17}$$

Specific consumption in Wh/km indicates how much energy a vehicle consumes per kilometre, which allows comparison of different scenarios and configurations.

Finally, estimated range of the vehicle is defined as the amount of usable energy in the battery divided by specific consumption ($spec$). A realistic estimate of the driving range based on the driving cycle is derived from the relationship between the range (in km) and the specific energy consumption:

$$range = \frac{E_{bat} \cdot f_{usable} \cdot 1000}{spec}, \tag{18}$$

where E_{bat} is the nominal battery capacity [kWh], f_{usable} is the usable share of the battery energy, and the factor 1000 converts [kWh] to [Wh].

2.5 Optimization Method

The optimization algorithm used in this study is the so-called DIRECT (Dividing RECTangles). DIRECT, which is a deterministic sampling method that is designed for bound-constrained non-smooth problems in a small number of variables. It is applicable to engineering design problems, in which complicated simulators are used to construct the objective function. Sampling occurs at the centers of hyperrectangles. In each iteration, the method divides existing hyperrectangles and then evaluates the objective function at the centers of the newly formed sub-hyperrectangles [37].

In this study, the DIRECT method is implemented in the MATLAB environment using WLTC 3b driving cycle data [38]. The maximum number of objective function evaluations and the number of iterations is limited to ensure reasonable computational complexity and simulation runtime. This method ensures that the found solution is sufficiently close to the global optimum, which is important considering the complexity of the electric vehicle model and the multiple conditions (range, power, charge/discharge rate (C-rate), SoC limits, performance point) that must be met.

2.6 Objective Function

In order to optimize parameters of an electric vehicle, it is necessary to define an objective function (J) which the algorithm minimizes. The objective function includes capital expenses (CAPEX), operating expenses (OPEX) and penalties that ensure that the vehicle meets the given conditions:

$$J = CAPEX + OPEX + penalties. \tag{19}$$

Vector of variables that are being optimized is defined as follows:

$$x = \left[E_{bat}\,[\mathrm{kWh}]\,, P_{max}\,[\mathrm{kW}]\,, m_{load}\,[\mathrm{kg}]\right], \tag{20}$$

where m_{load} is the useful vehicle payload.

Capital expenses depend on the battery capacity, the peak motor power and their prices:

$$CAPEX = c_{bat}E_{bat} + c_{motor}P_{max}, \tag{21}$$

where c_{bat} stands for the battery price, the price that is used in simulation is 120 EUR/kWh [39], and c_{motor} stands for the motor and inverter prices. The whole electric drive module costs around 570 EUR/kW [40]. The latter is a very conservative cost estimate, but realistic for the electrical motor plus inverter according to [40].

Operating expenses are calculated based on the estimated specific energy consumption during the cycle and the price of electricity:

$$OPEX = c_{el}\left(\frac{Wh/km}{1000}\right)N, \tag{22}$$

where c_{el} represents the price of electricity from the main utility grid, with the selected value in this study to be 0.2 EUR/kWh [41], and N is the reference distance in kilometers.

As shown above, CAPEX is linear, while OPEX represents the cost of energy at a given distance. The unit cost values are expressed in [EUR/kWh], [EUR/kW], [EUR/kWh_el]. They are in a realistic range, and they enable comparison between different configurations. The objective function is expressed in euros, but this does not represent the real market prices of the vehicle but serves as a comparative measure that equalizes the different contributions (battery, motor, energy consumption).

If the solution does not meet any of the conditions, the objective function is increased, adding a penalty and searching for a configuration that meets all the conditions. The conditions that are penalized are:

(a) Insufficient range (if less than the specified minimum)
(b) Insufficient motor power (if it is less than required)
(c) C-rate factor limitations (if the battery cannot deliver the required power)
(d) SoC limits (if the battery is too discharged)
(e) “Performance point” (the requirement that a vehicle overcomes a given slope at a certain speed)

The penalty terms used in the optimization are detailed in Table 1. To ensure a robust search process, quadratic penalization is applied to range violations to strongly discourage configurations that do not meet the primary mission requirement. Meanwhile, linear penalties are employed for power, C-rate, SoC, and performance constraints. This formulation is designed to preserve the smoothness of the objective function landscape, facilitating the convergence of the DIRECT algorithm while ensuring that all performance constraints are strictly respected.

Table 1: Penalty terms used in the optimization.

Penalty	Condition	Form
Range	$R_{est} < R_{min}$	Quadratic
Power	$R_{req} > R_{max}$	Linear
C-rate	$P_{out} > C_{rate,max} \cdot E_{bat}$	Linear
SoC	$SoC_{end} < SoC_{min}$	Linear
Performance	$P_{req,perf} > P_{max}$	Linear

By combining all mentioned expenses and penalties, the overall objective function takes the form:

$$J = CAPEX + OPEX + pen_{range} + pen_{power} + pen_{crate} + pen_{soc} + pen_{perf}, \tag{23}$$

where pen_{range}, pen_{power}, pen_{crate}, pen_{soc} and pen_{perf} are penalty factors related to insufficient range, insufficient motor power, C-rate factor limitations, SoC limit and performance point, as discussed above. Such an approach allows the optimization algorithm to search for the battery, motor and mass configuration that provides the best compromise between cost, energy efficiency and performance.

2.7 Optimization Framework

The optimization framework shown in Fig. 1 follows a sequential information flow starting from the driving cycle input, which provides the vehicle speed profile as a function of time. Together with the optimization variables and fixed vehicle parameters, the driving cycle is processed by the vehicle dynamics model to calculate the traction force and mechanical power demand. This power demand is then passed to the electric motor and inverter model, where electrical losses and power limitations are considered. The resulting DC power demand is supplied by the battery model, which computes the State of Charge (SoC) evolution and total extracted energy. Based on these results, the specific energy consumption and driving range are calculated. Finally, all relevant cost components and penalty terms are combined within the objective function, the value of which is minimized using the DIRECT optimization algorithm.

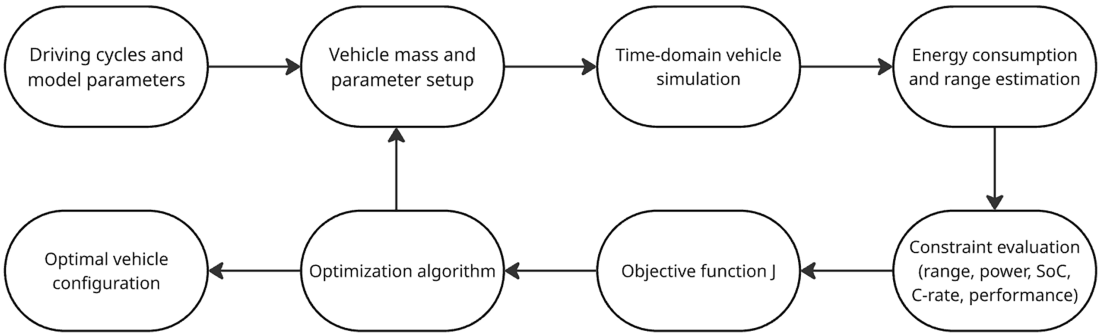

Figure 1: Block diagram of the proposed vehicle optimization approach.

3 Optimization Results

The optimization for both cars starts with these intervals: from 50 to 150 kWh (battery capacity), from 100 to 500 kW (peak motor power) and from 100 to 600 kg (vehicle useful payload). For each case study (Renault Zoe and Tesla Model 3), an optimization was performed using the corresponding technical parameters. The procedure identifies the optimal combination of battery capacity, motor power and payload that minimizes the cost function J. The results of the optimization are presented together with the WLTC simulation profiles (speed, power and SoC) for the obtained optimum.

3.1 Renault Zoe Optimization

For the Renault Zoe, the optimizer converged to E_{bat} = 52 kWh, P_{max} = 110 kW and m_{load} = 114 kg with an objective function value of J = 17,246 EUR. The WLTC simulation yields a specific consumption of 196 Wh/km and an estimated range of 238 km based on the usable battery energy (90% of nominal). The peak drivetrain output during the cycle is 49.6 kW, well below the installed P_{max}, indicating adequate performance margin and no power-limit penalty. The state of charge decreases from 0.95 to 0.85, remaining safely above the SoC minimum.

Fig. 2 shows the WLTC speed profile for Renault Zoe operating under WLTC driving cycle conditions. Fig. 3 shows the local sensitivity of the objective function J to three optimization variables for Renault Zoe: battery capacity (E_{bat}), peak motor power (P_{max}) and payload (m_{load}). It is visible that the battery capacity has the greatest impact on the value of the objective function, which is expected because it directly affects the investment cost, but it also directly affects the specific consumption and range of the vehicle. The peak power of the electric motor has a smaller impact, since the values of its maximum power are rarely required during the WLTC cycle. The smallest impact is shown by the additional load, although the increase in mass increases energy consumption and reduces the range.

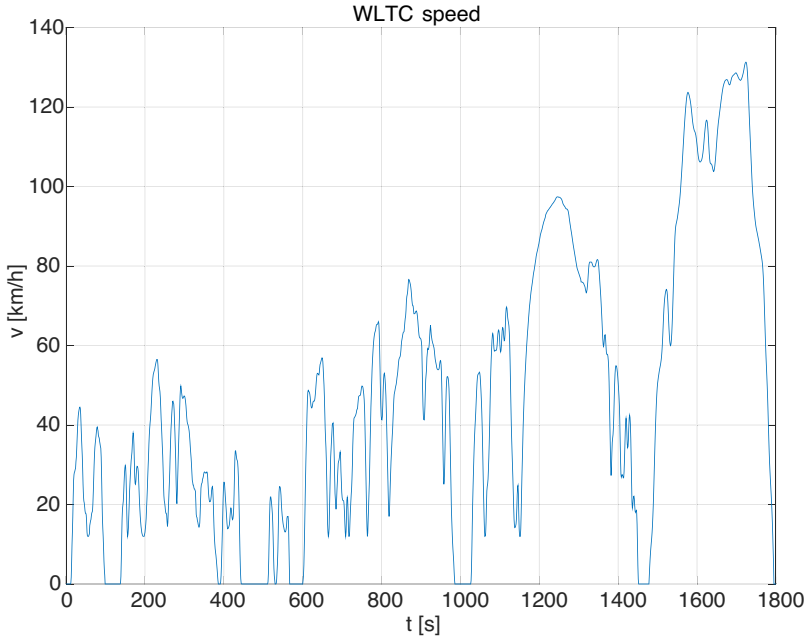

Figure 2: WLTC speed profile for Renault Zoe.

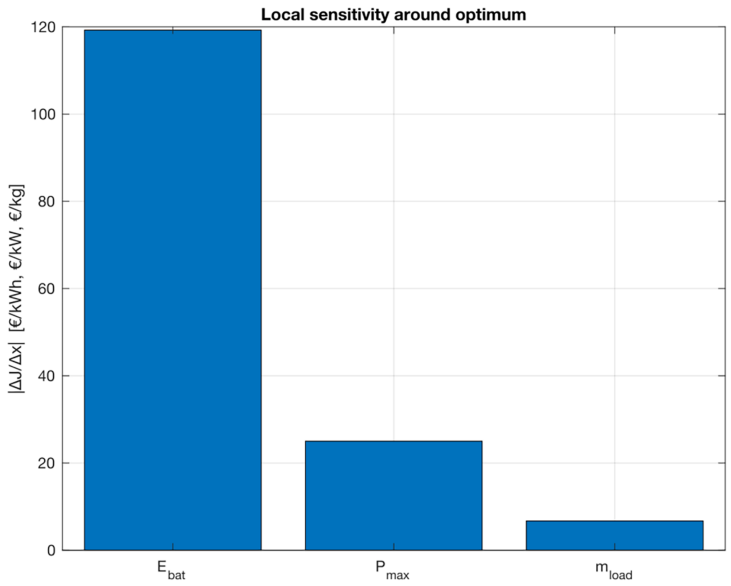

Figure 3: Local sensitivity around optimum for Renault Zoe.

Fig. 4 shows the contours of the objective function *J* for Renault Zoe as a function of the battery capacity (E_{bat}) and the peak power of the electric motor (P_{max}), with the load mass (m_{load}) fixed at the optimal value. The yellow dot indicates the optimal solution. It is noticed that the optimum is located to the left of the red line, which means that the vehicle in this case does not meet the minimum range requirement (300 km). However, this result is expected given all the losses included in the model (mechanical, electrical and auxiliary), which realistically reduce the effective range of the vehicle. This confirms the importance of introducing penalty conditions into the objective function, because the algorithm still finds the configuration that best balances costs and performance, even if some requirements (such as range) are not fully met.

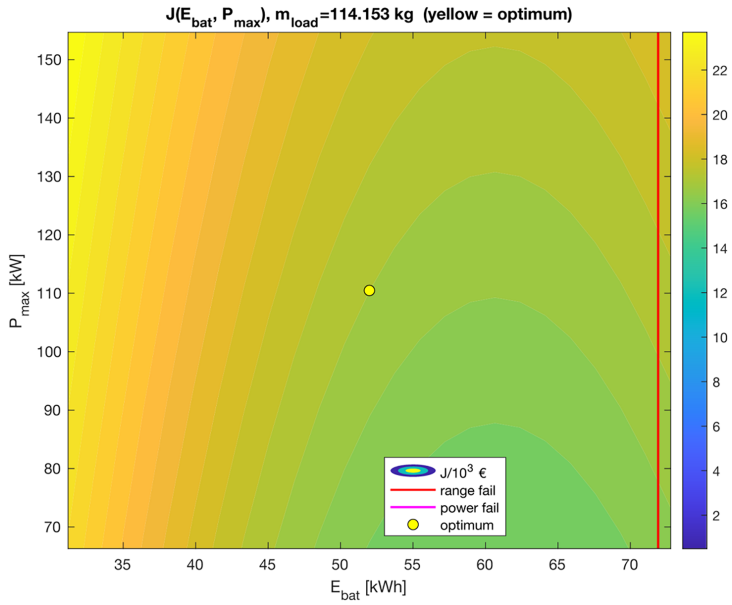

Figure 4: Contours of the objective function J for Renault Zoe as a function of the battery capacity (E_{bat}) and the peak power of the electric motor ($P_{\max}$), with the load mass (m_{load}) fixed at the optimal value.

Fig. 5 contains 3 graphs. The first graph (a) shows the vehicle speed over time, which corresponds to the driving cycle profile and varies from a standstill to approximately 130 km/h. The second graph (b) shows the motor output power ($P_{outpeak}$). During acceleration and driving at higher speeds, there are significant power spikes, while at rest and at low speeds, the demands are minimal. The third graph (c) shows the change over time in the battery state of charge (SoC). A gradual and almost linear discharge of the battery is visible over the duration of the cycle. The final SoC value at the end of the simulation is 0.85, confirming that the vehicle had sufficient energy available to meet the power demands throughout the cycle.

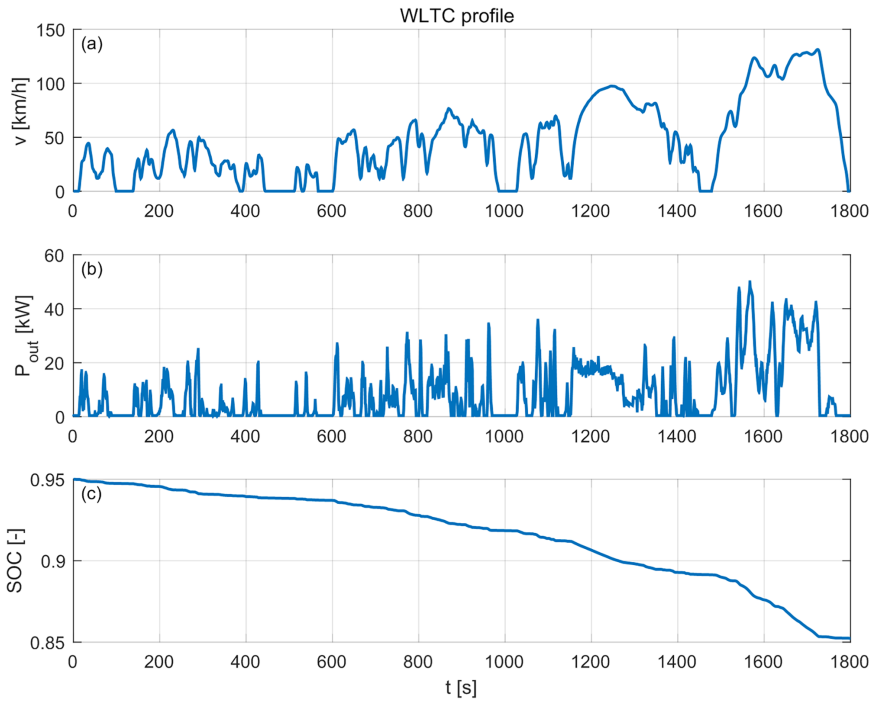

Figure 5: Renault Zoe velocity (**a**), power (**b**) and battery SoC (**c**) of WLTC cycle.

3.2 Tesla Model 3 Optimization

In the case of Tesla Model 3 vehicle, the optimizer converged to E_{bat} = 131.9 kWh, P_{max} = 128 kW and m_{load} = 120.939 kg with an objective function value of J = 27,041 EUR. The WLTC simulation yields a specific consumption of 227 Wh/km and an estimated range of 523 km based on the usable battery energy (90% of nominal). The peak drivetrain output during the cycle is 59.6 kW, well below the installed P_{max}, indicating adequate performance margin and no power-limit penalty. The state of charge decreases from 0.95 to 0.91, remaining safely above the SoC minimum.

Fig. 6 shows the local sensitivity of the objective function J to three optimization variables for Tesla Model 3: battery capacity (E_{bat}), peak motor power (P_{max}) and payload (m_{load}). It is visible that the peak power of electric motor (P_{max}) has the greatest impact on the value of the objective function. This means that the choice of peak motor power plays a crucial role in the balance between price, performance and energy consumption. On the other hand, the additional load (m_{load}) has a medium level of influence on the objective function, which makes sense because the increase in mass directly affects the energy consumption and thus the range. The smallest impact is shown by the battery capacity (E_{bat}), because the optimization is already in the area where an additional increase in capacity does not bring the proportional benefits.

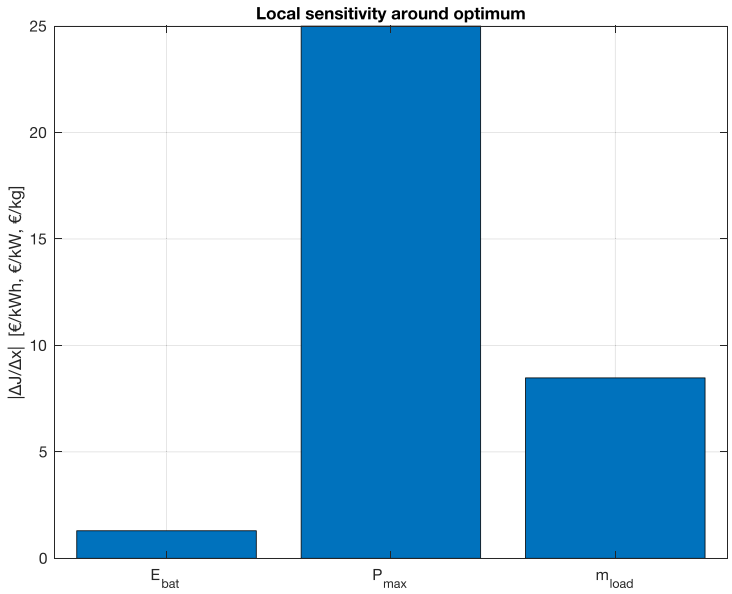

Figure 6: Local sensitivity around optimum for Tesla Model 3.

Fig. 7 shows the contours of the objective function J for Tesla Model 3 as a function of the battery capacity (E_{bat}) and the peak power of the electric motor (P_{max}), with the load mass (m_{load}) fixed at the optimal value. The yellow dot indicates the optimal solution. It is noticed that the optimum is located to the left of the red line, which means that the vehicle in this case does not meet the minimum range requirement (550 km).

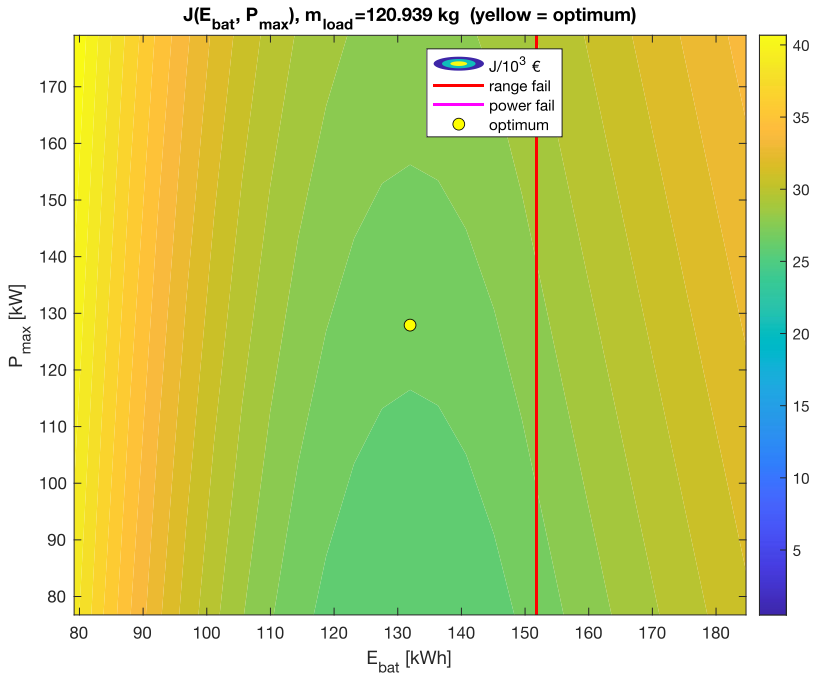

Figure 7: The contours of the objective function J for Tesla Model 3 as a function of the battery capacity (E_{bat}) and the peak power of the electric motor ($P_{\max}$), with the load mass (m_{load}) fixed at the optimal value.

However, this result is expected given all the losses included in the model (mechanical, electrical and auxiliary), which realistically reduce the effective range of the vehicle. This confirms the importance of introducing penalty conditions into the objective function, because the algorithm still finds the configuration that best balances costs and performance, even if some requirements (such as range) are not fully met.

Fig. 8 again contains 3 graphs. The first graph (a) shows the vehicle speed over time, which closely follows the driving cycle profile and varies from a standstill to approximately 130 km/h. The second graph (b) shows the motor output power ($P_{outpeak}$). During acceleration and driving at higher speeds, there are significant power spikes, while at rest and at low speeds, the demands are minimal. The third graph (c) shows the change over time in the battery state of charge (SoC). A gradual and almost linear discharge of the battery is visible over the duration of the cycle. The final SoC value at the end of the simulation is approximately 0.91, confirming that the vehicle had sufficient energy available to meet the power demands throughout the cycle.

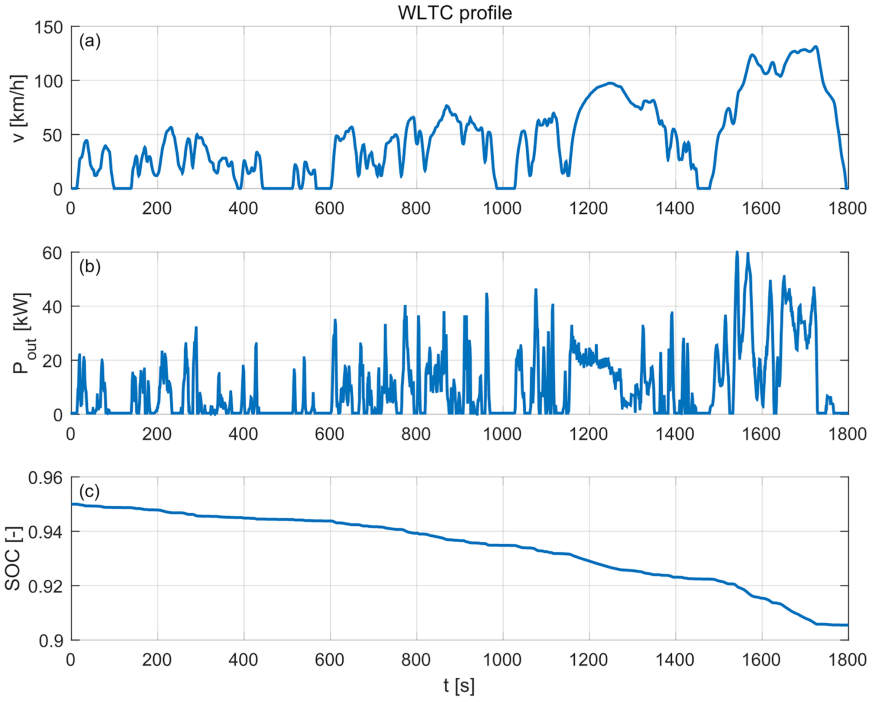

Figure 8: Tesla Model 3 velocity (**a**), power (**b**) and battery SoC (**c**) of WLTC cycle.

4 Discussion

The optimization results for Renault Zoe and Tesla Model 3 show clear differences in optimal vehicle configurations, which result from different initial parameters. For the Renault Zoe, the optimal solution includes a battery with a capacity of 52 kWh and a peak motor power of 110 kW, with an additional load of about 114 kg. The resulting range of 238 km and specific consumption of 196 Wh/km clearly show the limitations of a smaller vehicle with a smaller battery. Although the motor power meets the requirements of the WLTC cycle, the biggest drawback lies in the insufficient range. This is expected considering the relatively small battery capacity and additional losses of the model.

Fig. 9 illustrates the behavior of the objective function as a function of battery capacity for the Renault Zoe. A clear minimum is observed around E_{bat} = 52 kWh, confirming the optimal solution obtained by the optimization algorithm. For smaller battery capacities, the objective function increases rapidly due to range-related penalty terms, whereas for larger capacities the cost increase is dominated by higher battery

investment costs. Fig. 10 shows the evolution of the battery state of charge as a function of the driven distance over the WLTC cycle. The SoC decreases smoothly from the initial value of 0.95 to approximately 0.85 at the end of the cycle, remaining well above the minimum SoC constraint. This behavior confirms that the optimized configuration satisfies the energy and range requirements without approaching operational limits during a single driving cycle.

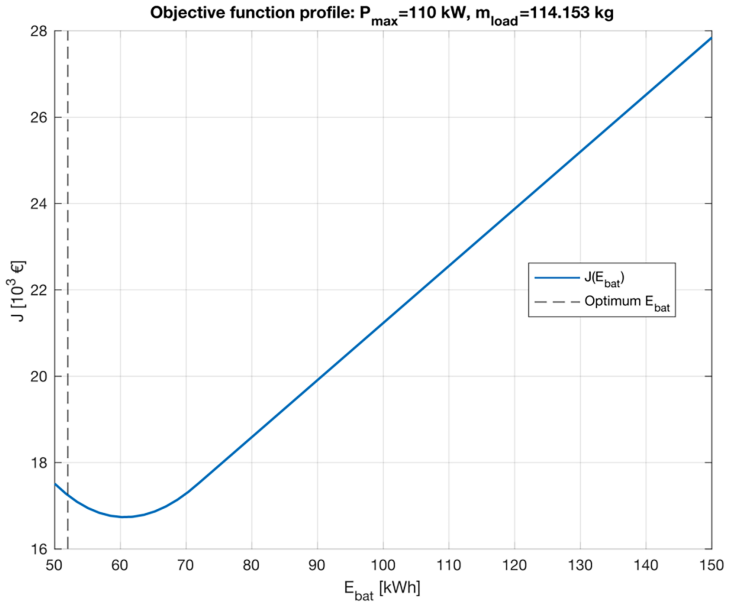

Figure 9: Objective function profile $J(E_{\text{bat}})$ for the Renault Zoe.

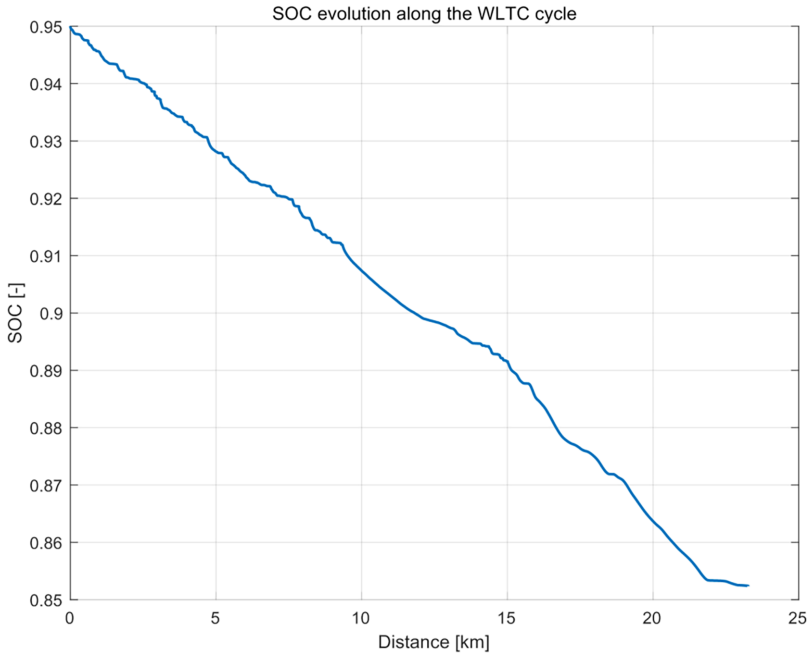

Figure 10: SoC evolution as a function of driven distance during the WLTC cycle for the optimized Renault Zoe configuration.

For the Tesla Model 3, the optimum was found at a battery capacity of 132 kWh, a peak motor power of 128 kW and an additional load of 121 kg. A range of 523 km was achieved with a specific consumption of 227 Wh/km. Unlike the Renault Zoe, the range penalty is not so pronounced here, because of the high battery capacity. However, the sensitivity analysis showed that the peak motor power has the greatest impact on the objective function. It affects cost the most because the battery has a high capacity, so it does not affect the objective function as much as the peak motor power. While for the Zoe, the battery capacity had the dominant impact.

Fig. 11 illustrates the dependence of the objective function on the battery capacity for the Tesla Model 3, while the motor peak power and additional load are kept fixed at their optimal values. The curve exhibits a well-defined minimum at approximately 132 kWh, indicating a clear trade-off between battery investment cost and operating cost. For lower battery capacities, the objective function increases sharply due to range and SoC related penalty terms, whereas for larger capacities the total cost rises primarily because of increased battery investment. Fig. 12 presents the evolution of the battery state of charge as a function of driven distance for the Tesla Model 3 case study. The SoC decreases gradually from the initial value of 0.95 to approximately 0.90 over the WLTC cycle, remaining well above the minimum SoC constraint throughout the entire drive. This confirms that the optimized configuration satisfies the imposed energy and range requirements with a substantial safety margin during a single standardized driving cycle.

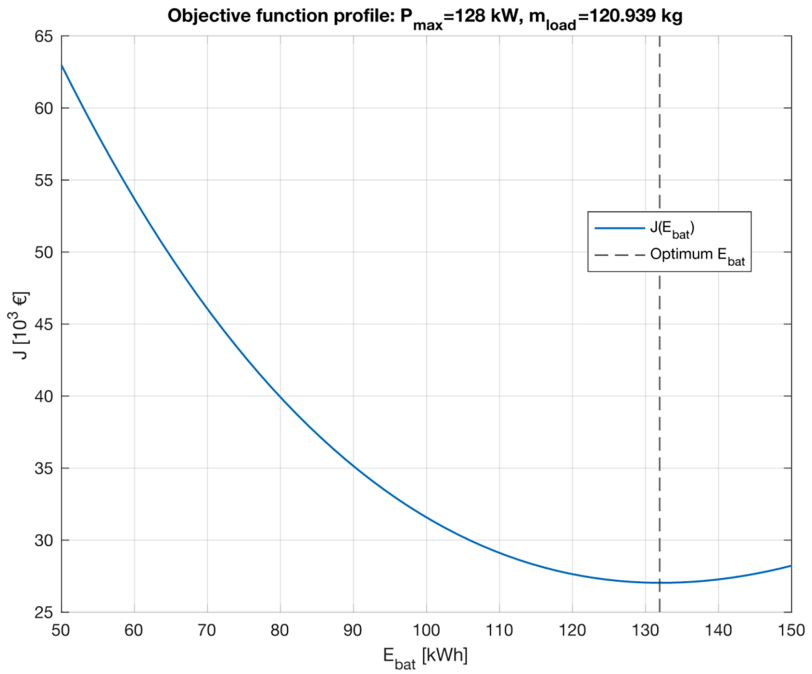

Figure 11: Objective function profile $J(E_{\mathbf{bat}})$ for the Renault Zoe.

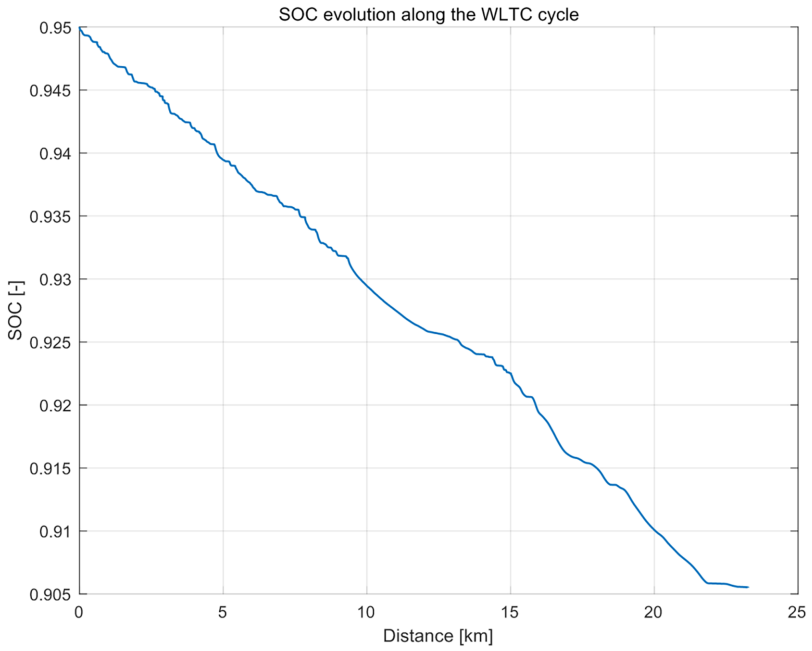

Figure 12: SoC evolution as a function of driven distance during the WLTC cycle for the optimized Tesla Model 3 configuration.

Comparative Analysis and Model Limitations

The optimization results for the Tesla Model 3 indicate a theoretical optimal battery capacity of approximately 132 kWh. While this exceeds the 50–82 kWh range found in commercial versions, it serves to illustrate the impact of the model's specific constraints. The objective function was configured to strongly penalize insufficient range, and the exclusion of regenerative braking increased the simulated net energy demand per kilometer. Under these conservative assumptions, the algorithm identifies a larger battery as the most effective solution to satisfy performance constraints and maintain a high SoC buffer. In industrial vehicle development, this capacity would be further 'trimmed' by physical packaging limits, cost-to-market targets, and the inclusion of energy recovery systems, factors that were intentionally excluded here to establish a conservative baseline for preliminary sizing.

The relatively small reduction in SoC (0.95 to 0.91 for the Tesla Model 3 and 0.95 to 0.85 for the Renault Zoe) is attributed to the short duration of the WLTC cycle (23.26 km) relative to the optimized ranges of 523 and 238 km, respectively. This narrow operational window ensures that the battery remains within its high-efficiency voltage plateau throughout the cycle, which is consistent with the goal of providing an adequate performance margin and avoiding power-limit penalties in a preliminary sizing study.

The observed higher energy consumption for the Tesla Model 3 (227 Wh/km) compared to the Renault Zoe (195 Wh/km) is a result of the model's physical scaling and the intentional exclusion of regenerative braking. Since battery mass is modeled as proportional to capacity, the optimized 132 kWh Tesla configuration is significantly heavier, leading to higher rolling resistance and inertial demand. Without the ability to recover kinetic energy during the frequent decelerations of the WLTC cycle, the heavier vehicle is penalized more severely than the lighter Zoe. Furthermore, the increased tractive effort required for the heavier vehicle elevates drivetrain losses, which scale quadratically with torque. These results highlight how conservative design assumptions (prioritizing range safety margins without the 'safety net' of recuperation) can lead to higher specific energy demands in preliminary sizing.

While the current study utilizes the WLTC due to its comprehensive inclusion of urban, suburban, and highway driving phases, we acknowledge that sensitivity to specific usage patterns could be further explored. The robustness of the presented configurations is currently ensured through strict constraint-based penalties on range and power. However, future extensions of this research will incorporate a wider variety of driving cycles to investigate how different regional driving behaviors or extreme congestion scenarios might further influence the optimal battery-to-motor sizing ratio.

5 Conclusion

In this paper, a computational model was created for parametric optimization of battery capacity, peak motor power and additional load for electric vehicles. The model was applied to two types of cars: Renault Zoe and Tesla Model 3. The model included vehicle dynamics, motor and converter losses, battery model and calculation of specific consumption and range, and the optimization was performed using the DIRECT method in the MATLAB environment.

The results show that the mutual influences of the parameters clearly differ depending on the size and characteristics of the vehicle. With the Renault Zoe, the key parameter was the battery capacity, because it largely determines the range of the vehicle. The reduced capacity leads to a penalty due to insufficient range, so the optimum was a result of a compromise between the battery price and the required range. With the Tesla Model 3, thanks to the larger battery capacity, the range penalty is not crucial, but the peak motor power has the greatest influence on the target function, because it ensures the ability to overcome performance requirements, especially incline and acceleration.

The influence of cost parameters on the optimal solution is indirectly assessed through local sensitivity analysis, which indicates that the overall optimization trends are robust with respect to moderate variations in cost assumptions.

In general, it can be concluded that battery capacity has a dominant influence on range and specific consumption. If the capacity is too low, it leads to high penalties. Motor power is crucial for meeting performance requirements and becomes a dominant factor in larger vehicles with higher battery capacity. Additional load has a linear, but smaller, impact on consumption and range compared to the previous two parameters. These results confirm that the optimal configuration of an electric vehicle is the result of a trade-off between range, power and cost. For city vehicles, the emphasis should be on increasing battery efficiency and reducing energy consumption, while for larger vehicles, optimization should focus on balancing drive power and battery capacity.

Acknowledgement: None.

Funding Statement: It is gratefully acknowledged that this research has been supported by the European Regional Development Fund under grant agreement PK.1.1.10.0007 (DATACROSS).

Author Contributions: The authors confirm contribution to the paper as follows: study conception and design: Ivan Pliško and Mihael Cipek; data collection: Ivan Pliško and Mihael Cipek; analysis and interpretation of results: Ivan Pliško, Mihael Cipek and Danijel Pavković; draft manuscript preparation: Ivan Pliško, Danijel Pavković and Mihael Cipek. All authors reviewed and approved the final version of the manuscript.

Availability of Data and Materials: Due to the nature of this research and confidentiality restrictions, participants of this study did not agree for their data to be shared publicly, so supporting data is not available.

Ethics Approval: Not applicable.

Conflicts of Interest: The authors declare no conflicts of interest.

Nomenclature

Abbreviations

CAPEX	Capital Expenses
DC	Direct Current
DIRECT	Dividing RECTangles (optimization algorithm)
EV	Electric Vehicle
GHG	Greenhouse Gas
NSGA-II	Non-dominated Sorting Genetic Algorithm II
OPEX	Operating Expenses
SoC	State of Charge
WLTC	Worldwide Harmonized Light Vehicles Test Cycle

Variables and parameters

$a(t)$	Vehicle acceleration
A	Frontal area of the vehicle
c_{bat}	Battery price
C_d	Aerodynamic drag factor
c_{el}	Price of electricity
c_{mot}	Motor and inverter price
E_{bat}	Nominal battery capacity
$E_{batt,out}$	Total energy drawn from battery
E_{cons}	Total energy consumption
F_{aero}	Aerodynamic drag force
F_{hc}	Hill climbing force
F_{inert}	Inertial force
F_{roll}	Rolling resistance force
F_{trac}	Traction force
f_{usable}	Usable share of battery energy
g	Gravitational acceleration
$I(t)$	Momentary battery current
J	Objective function
k	Time step index
k_{Cu}	Copper loss coefficient
k_{Fe}	Iron loss coefficient
k_{fric}	Constant mechanical loss coefficient
m	Total mass
m_0	Empty vehicle mass
m_{bat}	Battery mass
m_{load}	Payload/Load mass
N	Reference distance
P_{aux}	Auxiliary consumption
P_{dc}	DC power delivered by battery
P_{loss}	Power losses
P_{max}	Peak motor power
P_{mech}	Driveline mechanical power
P_{out}	Output drive power
pen_{crate}	Penalty: C-rate limitation
pen_{perf}	Penalty: Performance point
pen_{power}	Penalty: Insufficient power

pen_{range}	Penalty: Insufficient range
pen_{soc}	Penalty: SoC limit
Q	Battery charge capacity
s	Travelled distance
$spec$	Specific consumption
t	Time
T_m	Motor torque
v	Vehicle velocity
V_{nom}	Nominal voltage
Δt	Simulation time step
η_{inv}	Inverter efficiency
θ	Slope angle
μ_r	Rolling friction coefficient
ρ	Air density
ω_m	Angular velocity

References

1. Rimpas D, Barkas DE, Orfanos VA, Christakis I. Decarbonizing the transportation sector: a review on the role of electric vehicles towards the European green deal for the new emission standards. Air. 2025;3(2):10. doi:10.3390/air3020010.
2. Bansal M. The future of sustainable transportation: a comprehensive study of electric vehicle adoption and its impact on global carbon emissions. J Sust Sol. 2025;2(2):1–7. doi:10.36676/j.sust.sol.v2.i2.63.
3. Velho SRK, Vanderlinde ASG, Almeida AHA, Barbalho SCM. Electromobility strategy on emerging economies: beyond selling electric vehicles. Clean Energy Syst. 2024;9:100166. doi:10.1016/j.cles.2024.100166.
4. Sanguesa JA, Torres-Sanz V, Garrido P, Martinez FJ, Marquez-Barja JM. A review on electric vehicles: technologies and challenges. Smart Cities. 2021;4(1):372–404. doi:10.3390/smartcities4010022.
5. Zaino R, Ahmed V, Alhammadi AM, Alghoush M. Electric vehicle adoption: a comprehensive systematic review of technological, environmental, organizational and policy impacts. World Electr Veh J. 2024;15(8):375. doi:10.3390/wevj15080375.
6. Diouf B. The electric vehicle transition. Environ Sci Adv. 2024;3(2):332–45. doi:10.1039/d3va00322a.
7. Pollock J, Chong PL, Ramegowda M, Dawood N, Habibi H, Hou Z, et al. Battery electric vehicles: a study on state of charge and cost-effective solutions for addressing range anxiety. Machines. 2025;13(5):411. doi:10.3390/machines13050411.
8. Berjoza D, Jurgena I, Masek J. Changes in electric car energy consumption depending on mass. In: Proceedings of the International Scientific Conference Engineering for Rural Development; 2024 May 22–24; Jelgava, Latvia.
9. Alhanouti M, Gießler M, Blank T, Gauterin F. New electro-thermal battery pack model of an electric vehicle. Energies. 2016;9(7):563. doi:10.3390/en9070563.
10. Shah SB, Silwal B, Lehikoinen A. Effciency of an electrical machine in electric vehicle application. J Inst Engineering. 2016;11(1):20–9. doi:10.3126/jie.v11i1.14692.
11. Zhou B, Li Z, Wang H, Cui Y, Hu J, Jiang F. Design and optimization of an electric vehicle powertrain based on an electromechanical efficiency analysis. Processes. 2025;13(6):1698. doi:10.3390/pr13061698.
12. Ananganó-Alvarado G, Umaña-Morel I, Keith-Norambuena B. Reinforcement learning in electric vehicle energy management: a comprehensive open-access review of methods, challenges, and future innovations. Front Future Transp. 2025;6:1555250. doi:10.3389/ffutr.2025.1555250.
13. Zhu M, Qian K, Liu X. A three-time-scale dual extended Kalman filtering for parameter and state estimation of Li-ion battery. Proc Inst Mech Eng Part D J Automob Eng. 2024;238(6):1352–67. doi:10.1177/09544070231153440.
14. Liu C, Yang Y, Liao A, Zou Y. Adaptive-efficient DP algorithm for hybrid electric vehicle powertrain: balancing computational efficiency and accuracy. Mathematics. 2025;13(21):3503. doi:10.3390/math13213503.

15. Acar E, Jain N, Ramu P, Hwang C, Lee I. A survey on design optimization of battery electric vehicle components, systems, and management. Struct Multidiscip Optim. 2024;67(3):27. doi:10.1007/s00158-024-03737-7.
16. Kim K, Kim N, Jeong J, Min S, Yang H, Vijayagopal R, et al. A component-sizing methodology for a hybrid electric vehicle using an optimization algorithm. Energies. 2021;14(11):3147. doi:10.3390/en14113147.
17. Minchala-Ávila C, Arévalo P, Ochoa-Correa D. A systematic review of model predictive control for robust and efficient energy management in electric vehicle integration and V2G applications. Modelling. 2025;6(1):20. doi:10.3390/modelling6010020.
18. Chen J, Miao D, Dai Y, Ghadamyari M. Investigating the effects of the driving cycle and penetration of electric vehicles on technical and environmental characteristics of the hybrid energy system considering uncertainties. Energy Eng. 2022;119(5):1985–2003. doi:10.32604/ee.2022.021142.
19. Husain I. Electric and hybrid vehicles: design fundamentals. 3rd ed. Boca Raton, FL, USA: CRC Press; 2021.
20. Wong JY. Theory of ground vehicles. 5th ed. Hoboken, NJ, USA: John Wiley & Sons; 2022.
21. Renault Zoe ZE50 R110 (2019-2024) price and specifications—EV Database [Internet]. [cited 2026 Feb 1]. Available from: https://ev-database.org/car/1164/Renault-Zoe-ZE50-R110.
22. Renault zoe—battery design [Internet]. [cited 2026 Feb 1]. Available from: https://www.batterydesign.net/renault-zoe/.
23. Tesla mode 3 dimensions and weights [Internet]. [cited 2026 Feb 1]. Available from: https://www.tesla.com/ownersmanual/model3/en_cn/GUID-56562137-FC31-4110-A13C-9A9FC6657BF0.html.
24. A complete guide on electric car battery weight [Internet]. [cited 2025 Feb 1]. Available from: https://getevgas.com/electric-car-battery-weight/.
25. Beater P. Pneumatic drives: system design, modelling and control. Berlin/Heidelberg, Germany: Springer; 2007.
26. Car tyre size list by rim size [Internet]. [cited 2026 Feb 1]. Available from: https://www.michelin.co.uk/auto/car-tyre-sizes/.
27. How iron losses directly influence the selection of A BLDC motor [Internet]. [cited 2026 Feb 1]. Available from: https://www.portescap.com/en/newsroom/whitepapers/2022/10/how-iron-losses-directly-influence-the-selection-of-a-bldc-motor.
28. Guzzella L, Sciarretta A. Vehicle propulsion systems: introduction to modeling and optimization. Berlin, Heidelberg: Springer; 2013. doi:10.1007/978-3-642-35913-2.
29. CEC inverter test protocol: PV performance modeling collaborative (PVPMC) [Internet]. [cited 2026 Feb 1]. Available from: https://pvpmc.sandia.gov/modeling-guide/dc-to-ac-conversion/cec-inverter-test-protocol/.
30. Cipek M, Pavković D, Kljaić Z, Mlinarić TJ. Assessment of battery-hybrid diesel-electric locomotive fuel savings and emission reduction potentials based on a realistic mountainous rail route. Energy. 2019;173:1154–71. doi:10.1016/j.energy.2019.02.144.
31. Carlson RB, Wishart J, Stutenberg K. On-road and dynamometer evaluation of vehicle auxiliary loads. SAE Int J Fuels Lubr. 2016;9(1):260–8. doi:10.4271/2016-01-0901.
32. All electric vehicles in Europe: EV Database [Internet]. [cited 2026 Feb 1]. Available from: https://ev-database.org/#group=vehicle-group&renault=1&tesla=1&sh-s=1&rs-pr=10000_100000&rs-er=0_1000&rs-ld=0_1000&rs-ac=2_23&rs-dcfc=0_300&rs-ub=10_200&rs-tw=0_2500&rs-ef=100_350&rs-sa=-1_5&rs-w=1000_3500&rs-c=0_5000&rs-y=2010_2030&s=1&p=0-10.
33. Pavković D, Komljenović A, Hrgetić M, Krznar M. Experimental characterization and development of a SoC/SoH estimator for a $LiFePO_4$ battery cell. In: IEEE EUROCON 2015—International Conference on Computer as a Tool (EUROCON); 2025 Sep 8–11; Salamanca, Spain. p. 1–6. doi:10.1109/EUROCON.2015.7313708.
34. Battery capacity calculator [Internet]. [cited 2026 Feb 1]. Available from: https://eridehero.com/tool/battery-capacity-calculator/.
35. The Difference between useable and nameplate capacity in ESS—Valen Utilities [Internet]. [cited 2026 Feb 1]. Available from: https://valenutilities.com.au/the-difference-between-useable-and-nameplate-capacity-in-ess/0.
36. De Gennaro M, Paffumi E, Martini G, Manfredi U, Vianelli S, Ortenzi F, et al. Experimental test campaign on a battery electric vehicle: laboratory test results (Part 1). SAE Int J Altern Powertrains. 2015;4(2015–01-1167):100–14. doi:10.4271/2015-01-1167.

37. Finkel DE, Kelley CT. Convergence analysis of the DIRECT algorithm. Optimization Online. 2004;14(2):1–10. doi:10.1007/s10898-006-9029-9.
38. MATLAB central: driving cycle (Simulink Block) [Internet]. [cited 2026 Feb 1]. Available from: https://www.mathworks.com/matlabcentral/fileexchange/46777-driving-cycle-simulink-block.
39. "From $153 to $111 per kWh": an analysis of eMobility battery cost declines over the past three years—Mobility Portal [Internet]. [cited 2026 Feb 1]. Available from: https://mobilityportal.eu/analysis-emobility-battery-cost/.
40. Slowik P, Isenstadt A, Pierce L, Searle S. Assessment of Light-duty electric vehicle costs and consumer benefits in the United States in the 2022-2035 time frame [Internet]. Washington, DC, USA: White paper of International Council on Clean Transportation; 2022 [cited 2026 Feb 1]. Available from: https://theicct.org/wp-content/uploads/2022/10/ev-cost-benefits-2035-oct22.pdf.
41. Eurostat: electricity price statistics, statistics explained [Internet]. [cited 2026 Feb 1]. Available from: https://ec.europa.eu/eurostat/statistics-explained/index.php?title=Electricity_price_statistics.